

DESIGN OF A HIGHLY OPTIMISED VACUUM CHAMBER SUPPORT FOR THE LHCb EXPERIMENT

L. Leduc, G. Corti, R. Veness, CERN, Geneva, Switzerland

Abstract

The beam vacuum chamber in the LHCb experimental area passes through the centre of a large aperture dipole magnet. The vacuum chamber and all its support systems lie in the acceptance of the detector, so must be highly optimised for transparency to particles. As part of the upgrade programme for the LHCb vacuum system, the support system has been re-designed using advanced lightweight materials. In this paper we discuss the physics motivation for the modifications, the criteria for the selection of materials and tests performed to qualify them for the particular environment of a particle physics experiment. We also present the design of the re-optimised support system.

INTRODUCTION

The conical shape of the beampipe in LHCb leads to unbalanced atmospheric forces in the axial direction, compensated at two fixed points, called S2F and S3F (see Figure 1). At each fixed point, the support system consists of a set of eight stainless steel wires and rods, designed to limit the axial displacement of the conical chamber and to provide enough stiffness in all transverse directions. The two wire systems are attached to aluminum collars, connected to the beampipe by graphite reinforced Vespel interface rings.

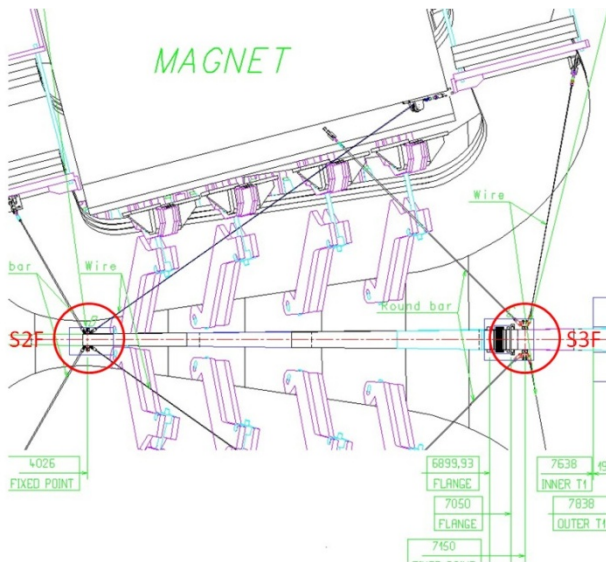


Figure 1: LHCb beampipe support system layout at the fixed points S2F and S3F.

The design of the vacuum chamber is particularly delicate in the LHCb experiment [1] since it is focussed on the high rapidity region, where the particle density is high. The probability of interesting particles interacting with elements of the vacuum chamber and the number of

secondary particles produced depends on the amount of material seen by incident primary particles. The mass of the vacuum chamber, the presence of flanges and bellows and of its support system have a direct influence on the occupancy, in particular of detectors close by. Optimization of the design and selection of materials were therefore performed in order to maximize transparencies in these critical regions [2,3] and led to the system currently installed in the experiment.

Despite this first optimization, the vacuum chamber support system has been identified as a major remaining source of background that as a result requires further consolidation.

A new design which minimizes the volume and uses materials with higher radiation length is presented here. It is shown to be feasible to replace the existing stainless steel rods with carbon fibre reinforced plastic tubes and use synthetic ropes instead of stainless steel cables, leading to an increase of transparency of more than 90%, while keeping enough stiffness. Replacing aluminium by beryllium for the collar leads to a transparency increase of more than 85%.

WIRE SYSTEM OPTIMIZATION

Material Selection Criteria

Two criteria are used for the material selection. First, the stiffness of the new solution must be high enough to limit the axial displacement of the chamber to less than 2 mm. Second, the radiation length of the material used should be high enough to allow a gain in transparency of the system. The indicator of a wire transparency can be related to the distance seen by the particle d , which can be either the diameter of the rope or twice the wall thickness of the tube, and the radiation length X_0 :

$$I_1 = \frac{d}{X_0} \quad (1)$$

Rigid Wires

An effective solution to replace the 8mm diameter rigid stainless steel rods consists of filament winding carbon fibre reinforced epoxy tubes, with 14 mm inner diameter and 17 mm outer diameter and 60% volume fraction of fibers, manufactured by Mateduc composites. The lay-up is defined as follow: [+8°/90°/-8°/+8°/90°/-8°]. Toray M46J carbon fibres are used for the 8° orientation, since they combine high strength and high modulus. T700 fibres are used for the compacting layers with 90° orientation fibres. The epoxy resin used is UF3325 TCR. The resultant radiation length is $X_0=230$ mm.

Flexible Wires

The current 3 mm diameter stainless steel 7x7 cables are replaced with synthetic ropes. Following a review of ropes available in the market, especially for sailing applications, Vectran and Technora materials were selected. Mechanical testings have been performed on the two types of ropes which led the following selection of ropes:

- 5 mm diameter Vectran HT fibre rope, 16 plies;
- 5 mm diameter Technora fibre rope, 12 plies.

Although the exact chemical formula of the two ropes are not available, a minimum and maximum value can be obtained by varying the fraction of each monomer constituents of the molecule: $289 \text{ mm} \geq X_0 \geq 294 \text{ mm}$ for Vectran and $X_0 \approx 297 \text{ mm}$ for Technora.

An advantage of the rope is that it can be terminated by a spliced eye at the beampipe side, which increases the transparency.

Transparency Increase of the New Wire System

Table 1 collects the radiation length of each type of wire of the current and new supports as well as the related transparency indicator. The results show that the transparency is greatly increased in the new supports:

- a 97% increase in transparency is found for the rigid wires;
- a 90% increase in transparency is found for the flexible wires.

Table 1: Transparency of the Current and New Support

| | Radiation length X_0 (mm) | I_1 |
|-------------------------|--------------------------------|---------|
| Current supports | | |
| - Rods | 17.6 | 0.45 |
| - cables | 17.6 | 0.17 |
| New supports | | |
| - CFRP | 230 | 1.3e-2 |
| tubes | >289 | <1.7e-2 |
| - Ropes | | |

Mechanical Performance of the New System

As shown in Table 2, the new system consistently has lower stiffness than the current one. This is due to the carbon fibre tube size. The outer diameter should not be too large in order avoid enlarging the termination at the beampipe side and the inner diameter is fixed by the manufacturers available mandrills. Despite this, the axial displacements of the beampipe are still acceptable. The stress safety factors confirm the feasibility of the solution, where for each wire the stress safety factors is calculated by dividing the stress by the ultimate stress of the wire.

Further Tests

Further tests are currently under investigation in order to predict the lifetime of the solution. First, the ropes need to be tested against radiation damage. However, it is

Table 2: Mechanical Performance of the Current and New Supports

| | Axial displacement | Stress safety factor |
|--------------------|--------------------|----------------------|
| S2F support | | |
| - Current | 1.2 | 25 |
| - New | 1.4 | 16 |
| S3F support | | |
| - Current | 0.75 | 2.9 |
| - New | 0.98 | 3.8 |

expected that Technora behaves similarly to Kevlar under radiation. Kevlar shows sufficient radiation resistance to LHCb total doses [4]. According to the manufacturer Kuraray, the polymer used to manufacture Vectran fibres have been tested up to 5 MGy gamma radiation, without noticeable degradation. Second, creep tests need to be performed on both the ropes and the bond between the carbon tube and terminations. An estimate of the creep behaviour of the ropes can be found in literature, see e.g. [5-6] but the lifetime can also be accurately predicted using a stepped isothermal method, based on time superposition concepts, i.e. accelerating the creep process by increasing the temperature, see [7].

COLLAR OPTIMIZATION

Material Selection

A full metallic solution is feasible in the case of the collar, leading to an improved transparency: beryllium offers an increased radiation length $X_{0Be} = 353 \text{ mm}$, compared to the aluminium radiation length, $X_{0Al} = 70 \text{ mm}$. However, Beryllium is brittle and toxic leading to safety issues. Mechanically, increased safety factors are included to cope with its brittleness, as well as a protective coating to prevent corrosion.

Among the available beryllium grades, the instrumental grade is selected for this application since it offers good mechanical strength.

Volume Optimization

In addition to the choice of material, the volume itself has also been minimized as shown on Figure 2 representing the current and new collar design of the S3F fixed point. In the previous design, an aluminium attachment system connects a rod and a cable to the collar (see Figure 2a). The attachment system is then fixed to the collar with stainless steel screws. The new design has an integrated attachment system. The volume of the attachment system is thus reduced and the use of stainless steel screws avoided.

Mechanical Performance of the New Collar

Finite elements analyses using Ansys have been performed, showing that the new design ensures comfortable stress safety factors as shown on Table 3.



Figure 2: current collar design (left) and new collar design (right) for S3F fixed point.

Table 3: Stress Safety Factor and Transparency of the Current and New Collars

| | Stress safety factor | I_2 |
|-------------------|----------------------|--------|
| S2F collar | | |
| - Current | 2.1 | 0.34 |
| - New | 4.2 | 4.5e-2 |
| S3F collar | | |
| - Current | 2.5 | 0.57 |
| - New | 3.6 | 8.5e-2 |

Increase in Transparency

The indicator of transparency can be taken of the form:

$$I_2 = \frac{t}{X_0} \quad (2)$$

where t is the thickness of the collar and X_0 the radiation length of the material. Table 3 compares the transparency of the current and new S2F and S3F collars. It is shown that the transparency is increased by 87% for S2F support and by 85% for S3F support.

INTERFACE RING OPTIMIZATION

Figure 3 shows the drawing of half the current Vespel ring clamping the beampipe to the collar. The symmetric parts of the interface ring are connected by stainless steel fasteners.

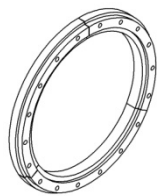


Figure 3: Drawing of half the current S3F interface ring.

An optimization has been made for the fasteners close to the beampipe. A noticeable gain is obtained by replacing the stainless steel fasteners, for which the radiation length is 17.6 mm, by titanium, with radiation length 35.6 mm. The number of fasteners is also decreased, leading to a volume reduction of the metallic fasteners of 75% for S2F and 62% for S3F.

The ring itself is also optimized. First, Celazole PBI is used instead of Vespel SP21. The radiation length of Celazole is calculated to be 304 mm, compared with 270mm for Vespel. In addition, Celazole PBI offers improved mechanical strength at 250°C, and thus could

be used during the bakeout of the chamber. By reducing the thickness of the ring, the volume of the ring itself decreases by 55% for S2F and 32% for S3F.

CONCLUSIONS

The new design allows an increased transparency of the key parts of the support system, namely the wires, the collar and associated attachment system, and the interface ring. It has been shown that replacing the current stainless steel rods by carbon fibre tubes gives an increase of transparency of 90%. Using synthetic ropes instead of the current stainless steel cables allows to have a 97% gain in transparency. In addition, the new design of collars with a large volume reduction, and using beryllium instrument grade leads to an increase of transparency of more than 85%. Finally, the interface ring and related fasteners have also been optimized by using lighter materials and volume optimization.

ACKNOWLEDGEMENTS

The authors are thankful to the technical support of J.G. Chauré and the guidance of M.A. Gallilei. They also wish to acknowledge M. Guinchard, T Dijoud for the measurements and S. Clément for assistance in gluing the carbon tubes. Thanks also to E. Anderssen for his help in designing the CFRP tube and the technical team of the TE/VSC-EIV section for their advice.

REFERENCES

- [1] The LHCb collaboration, “The LHCb Detector at the LHC”, 2008 JINST 3 S08005, Aug. 2008.
- [2] J.R. Knaster, “The vacuum chamber in the interaction region of particle colliders: a historical study and developments implemented in the LHCb experiment at CERN”, Ph.D. Thesis, CERN-ETSH, 2004.
- [3] D. Ramos, “Design of the fixed beampipe supports inside the acceptance region of the LHCb experiment”, <https://emds.cern.ch/documents/882924>.
- [4] P. Beynel, P. Mayer and H. Schönbacher, “Compilation of radiation tests data-part 3”, CERN 82-10, 1982.
- [5] R.B. Fette and M.F. Sovinski, “Vectran Fiber time dependent behaviour and additional static loading properties”, NASA/TM-2004-212773.
- [6] G.M. Fallatah, N. Dodds and A.G. Gibson, “Long term creep and stress rupture of aramid fibre”, Plastic, Rubber and Composites 36(9), pp. 403-412, 2007.
- [7] I.P. Giannopoulos, C.J. Burgoyne, “SIM test results for aramid fibres”, ACMBS-V, Winnipeg, Manitoba, Canada 2008.